LAWRENCE
LIVERMORE
NATIONAL
LABORATORY

LLNL-PROC-678399

Morphology of ejected debris from laser super-heated fused silica following exit surface laser-induced damage

S. G. Demos, R. A. Negres, M. D. Feit, K. Manes, A. M. Rubenenchik

October 20, 2015

XLVII Annual Symposium on Optical Materials for High-Power Lasers
Boulder, CO, United States
September 27, 2015 through September 30, 2015

Disclaimer

Morphology of ejected debris from laser super-heated fused silica following exit surface laser-induced damage

Stavros G. Demos, Raluca A. Negres, Rajesh N. Raman, Michael D. Feit,
Kenneth R. Manes, Alexander M. Rubenchik
Lawrence Livermore National Laboratory, 7000 East Ave., Livermore, CA 94551, USA

ABSTRACT

Laser induced damage (breakdown) initiated on the exit surface of transparent dielectric materials using nanosecond pulses creates a volume of superheated material reaching localized temperatures on the order of 1 eV and pressures on the order of 10 GPa or larger. This leads to material ejection and the formation of a crater. The volume of this superheated material depends largely on the laser parameters such as fluence and pulse duration. To elucidate the material behaviors involved, we examined the morphologies of the ejected superheated material particles and found distinctive morphologies. We hypothesize that these morphologies arise from the difference in the structure and physical properties (such as the dynamic viscosity and presence of instabilities) of the superheated material at the time of ejection of each individual particle. Some of the ejected particles are on the order of 1 μm in diameter and appear as "droplets". Another subgroup appears to have stretched, foam-like structure that can be described as material globules interconnected via smaller in diameter columns. Such particles often contain nanometer size fibers attached on their surface. In other cases, only the globules have been preserved suggesting that they may be associated with a collapsed foam structure under the dynamic pressure as it traverses in air. These distinct features originate in the structure of the superheated material during volume boiling just prior to the ejection of the particles.

Keywords: Fused Silica, laser-induced damage, laser superheated material.

1. INTRODUCTION

The use of high power/intensity laser pulses to deposit energy and modify solid state materials is continuously expanding. The laser energy is coupled into the material to generate localized high temperatures and pressures while the material becomes thermodynamically unstable. The ensuing material response is associated with an explosive process that leads to material removal and mechanical damage of the surrounding volume.

Measurements of dynamic parameters of these explosive processes such as the expansion of the shockwave and the ionized gas, and kinetics and distribution of ejected and re-deposited particles as a function of laser parameters and energy deposited have provided insight into the dynamics of the generated ejection plume [1-8]. Experimental evidence and modeling suggest that the material is exposed to pressures on the order of 10 GPa and temperatures on the order of 1 eV [9-12]. Much less information exists on the relaxation of this metastable state, and in particular, the dynamics and mechanisms involved in the relaxation of the superheated material. The relaxation process may include vaporization, particle ejection, radiative cooling and phase transformation. This is a complex problem that is very challenging to be described in detail using current modeling tools.

In the field of laser damage, the coupling of the laser energy to the optical material is unintentional and facilitated by the presence of some sort of absorbing defect but the ensuing physics is analogous to the general case. The process creates a volume of superheated material at near solid density that exhibits extreme gradients of temperature and thermo-physical property values while relevant phase diagrams are not known. It is characteristic that by creating damage on the exit surface of an optic, the plasma front expands towards the bulk (upstream the laser beam), thus creating the proper conditions to generate a larger volume of superheated material that can aid execution of experiments to study its transient properties. The physics involved in this process, at the boundaries on warm dense mater regime, is not well understood, although it is of fundamental importance for all related fields of use.

We have recently presented work related to the relaxation of laser superheated (via ns pulses) fused silica suggestive that the relaxation process involves a number of distinct phases which include the delayed explosive ejection of micro scale particles for a duration on the order of 1 μs after the pressure of the superheated material is reduced to about 4 GPa [13].

*Corresponding author: demos1@llnl.gov

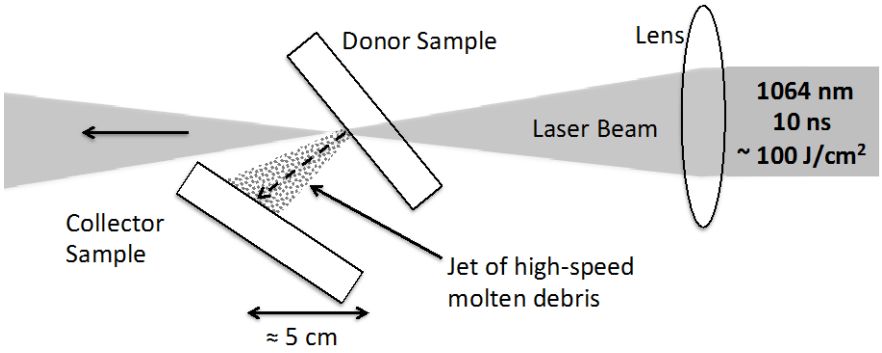

Figure 1. Experimental setup depicting the damage debris collection geometry optimized to facilitate the collection of molten debris within the formed jet of high speed ejected particles in ambient conditions.

The present work focuses on providing a more detailed characterization of the ejected particles as means to probe the transient structure of the superheated material in fused silica. Specifically, we hypothesize that after capturing the ejected debris generated during exit surface damage in fused silica, we can correlate the varying morphology of the debris with their ejection time and state of the material at the time of ejection. This in turn can help develop a better understanding of the relaxation process and dominant mechanisms and origin of the structural features of the resulting material modifications. In addition, this work helps better understand the impact on adjacent optical elements that may be in the path of the ejected particles during damage initiation or growth.

2. EXPERIMENTAL ARRANGEMENT

A schematic diagram of the experimental setup is shown in Figure 1. In brief, damage on the exit surface of a "donor" fused silica plate was induced using 1064 nm, 10 ns FWHM (full-width-half-maximum intensity) laser pulses having estimated peak fluence on the exit surface on the order of 100 J/cm^2. The beam was focused using a 10 cm focal length lens about 5 mm behind the exit surface of the donor sample to ensure damage initiation on the exit surface but not on the front surface or inside the bulk. The donor sample was positioned at an angle of about 45 degrees with respect to the direction of laser beam propagation so that the resulting jet of particles (always formed in a direction orthogonal to the exit surface plane) is offset from the laser beam propagation direction. This jet was subsequently intercepted by a second fused silica (the "collector") plate having its surface nearly parallel to the surface of the donor sample while separated by a distance of about 5 cm and shifted to avoid exposure to the pump laser beam. As a result, the molten debris (within the particle jet) is collected on the upper quadrant of the collector sample. All experiments were performed in ambient air.

A "cloud" of debris was observed after each laser exposure extending about 15 cm away from the donor sample. This cloud of debris was observed to follow the air-flow in the laboratory environment. Thus, particles from the debris cloud would also settle on other, more remotely placed collector samples, however those collected debris had primarily the appearance of mechanically fragmented silica rather than melted material following exposure to high temperatures/pressures. The configuration depicted in Figure 1 was chosen after attempting various particle collection geometries as it favored the collection of debris that has been exposed to high temperatures and melting exhibiting a plurality of morphologies (as revealed by SEM) within a region of about 1 cm in diameter in addition to the fragmentation debris over the entire surface of the collector sample.

3. EXPERIMENTAL RESULTS

Recent work [13] by our research team proposed that, following the superheating of a material volume via a laser pulse under excitation conditions similar to those presented in this work, the material relaxation process includes four discrete phases giving rise to ejected material with distinctive morphologies. These phases along with their estimated pressure range/duration include:

1) Surface explosion inducing the shock and gaseous material ejection. (Pressure: ≈ 10 → 4 GPa, Delay: 0 → ≈30 ns)
2) Delayed eruption of subsurface-confined superheated material (Pressure: ≈4 → 0.09 GPa, Delay: ≈30 → 80 ns)
3) Ejection of liquid material until thermodynamically stable liquid phase is reached (Pressure: ≈ 90 → 0.4 MPa, Delay: ≈80 → 1000 ns)
4) Ejection of mechanically damaged material due to stress (Pressure: < ≈0.6 MPa, Delay: >1000 ns)

Microscopic particles are ejected only during phases-2, -3 and -4 while the speed of the particles declines as the pressure and temperature of the superheated material decreases.

Figure 2 shows the speed of the ejected particles and corresponding pressure of the superheated material as a function of the time of ejection (delay from the pump pulse) as presented in [13]. During the relaxation, the temperature of the superheated material declines until a thermodynamically stable liquid phase is reached (at about 3100 K). Previous work [14] was suggestive that the temperature of ejected particles can be as high as about 5500 K. Thus, we consider that the temperature of the superheated material during the material ejection process is in the range between about 6000 K and 3000 K. Consequently, the viscosity of the material continuously changes with time during the ejection process. This in turn should affect the spatial characteristics of the melted debris. The work of Doremus [15] provides a good approximation of the viscosity of silica at the relevant temperatures range. Accordingly, the debris was categorized in 4 types (Type-1, -2, -3 and -4) based on their physical characteristics. The type-1 debris correspond to the particles ejected during phase-2. These particle are small in size (as it has been demonstrated in previous time resolved imaging studies) [16-17] and have speed between about 2.5 km/s and 300 m/s. Type-2 debris correspond to the particles ejected during phase-3 and are larger in size molten particles having speeds between about 300 m/s and 30 m/s following their ejection from the superheated material. Type-4 debris are associated with mechanically damaged (pulverized) "cold" material surrounding the superheated material volume while type-3 debris include mechanically damaged material at the boundaries of the melted material pool, thus including in part some molted material. The ejection speed of type-3 and -4 debris is less than about 30 m/s.

Representative examples of type-1 debris are shown in Figure 3. They have the appearance of small liquid droplets having diameter on the order of 2 μm or less. Two or more attached droplets are often observed generating more complex shapes. These particles were ejected during the explosive release of the confined superheated material (phase-2) and due to their low viscosity (expected to be motor oil to maple syrup like), the surface tension governs the shape of the particles leading to nearly spherical particles. A fiber "tail" (or remnants of that) with diameter on the order of 100 nm is often observed that was formed during the separation from the liquid pool. Often the particles have a partial appearance of splats, indicative that they have reached the collector sample while still largely in liquid phase. As it has been discussed previously [14], these hot ejected particles rapidly form a shell of colder material in the outer surface aided by evaporative cooling but their interior remains hot. This shell halts the evaporative cooling process and the interior is slowly cooling thereafter via heat conduction which has a much slower cooling rate. This enables the interior of these particles to remain very hot. On the other hand, the very narrow fibers formed during material separation cool down fast and can survive the flight through the air and impact on the collector sample.

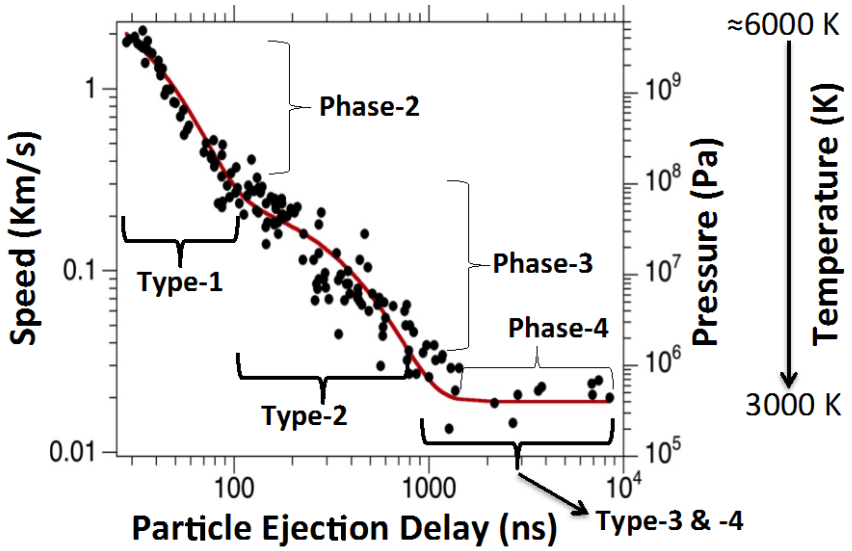

Figure 2. The speed of the ejected particles and corresponding pressure of the superheated material as a function of the delay time (from the pump pulse) of ejection of particles from the laser superheated material pool formed inside the surface of fused silica. The three phases of the material ejection process involving microscopic particles in correlation to the four types of particles ejected is also shown.

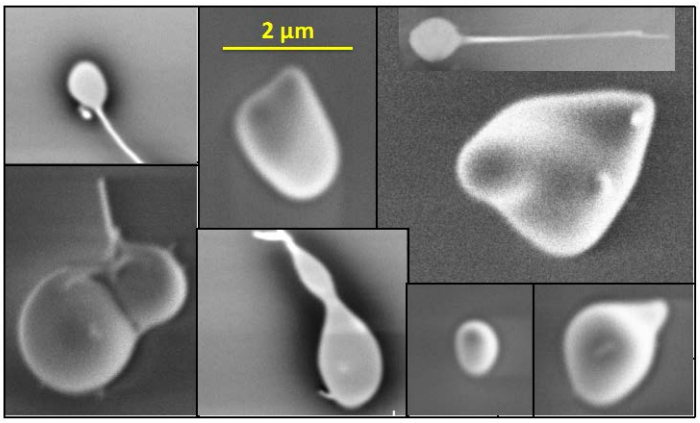

Figure 3. Representative SEM images of type-1 debris

Type-2 debris is formed during phase-3 of the ejection process. During this phase, the temperature changes significantly, from about 5000 K to about 3000 K, and the corresponding viscosity changes from maple syrup like to honey like. In addition, the dynamic pressure during the flight of the particle in air changes by two orders of magnitude (as the speed varies from about 300 m/s to 30 m/s), thus affecting the shape of the particle in liquid phase (which can be modified). Thus, we categorized the type-2 debris into three subgroups, type-2a, type-2b and type-2c. Representative examples are shown in Figs. 4a, 4b and 4c, respectively.

Type 2c debris is ejected at the later stage of phase-3. Due to the lower dynamic pressure they encounter, type-2c debris better maintain the structure of the particle at the time of separation from the superheated material. Representative examples shown in Figure 4c demonstrate stretched foam like structure, which may correspond to the network of bubbles formed inside the superheated material during volume boiling, thus capturing the complex morphology of the superheated material. The structure is characterized by globules (≈3 to 4 µm in diameter) and interconnecting columns

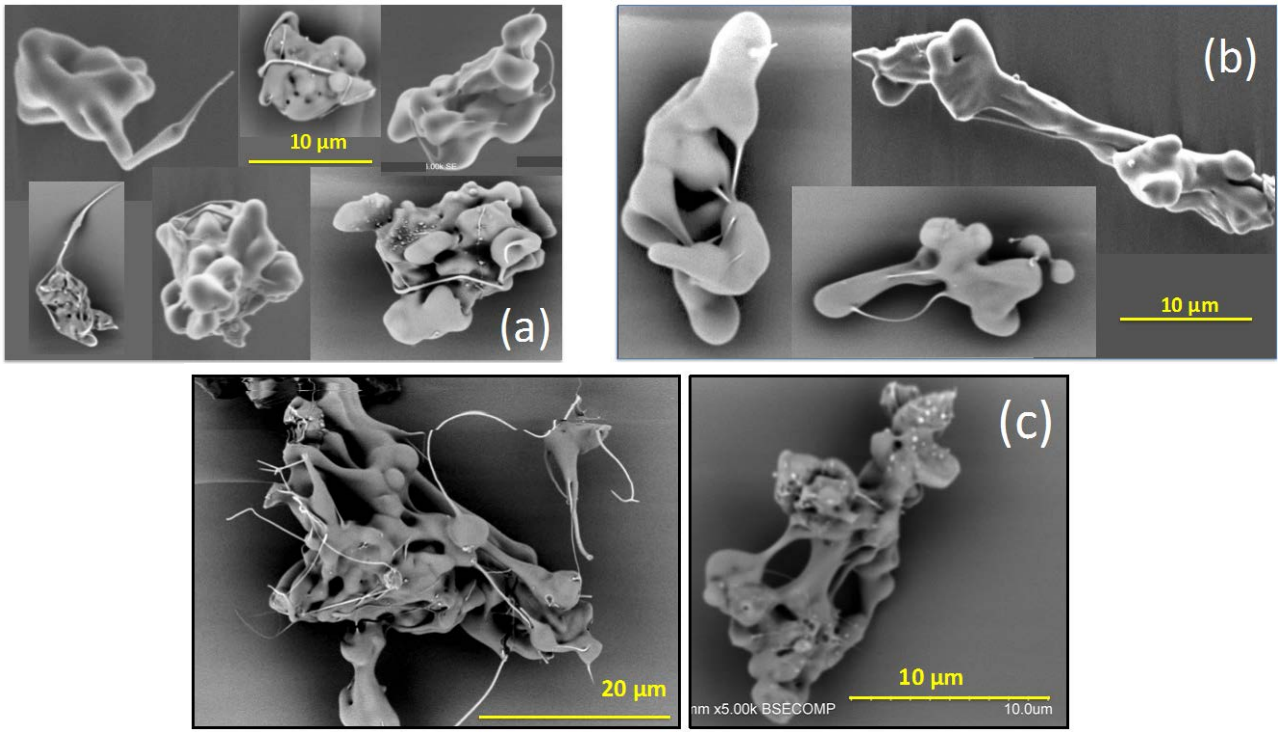

Figure 4. SEM images of type-2 debris. Due to the large spectrum of debris sizes and morphologies, they are categorized in to three subgroups, type-2a, type-2b and type-2c, shown in (a), (b) and (c), respectively.

(≈ 1 to 2 μm in diameter). Multiple fibers originating from different parts of the particle are commonly observed. It must be noted that these larger type-2c particles (20-40 μm in diameter) were possible because of the large pool of superheated material generated under the excitation conditions used in the experiments. Such particles may not be observed in damage sites generated under ICF class laser excitation conditions. However, they provide insight into the possible structure of the superheated material at the later stage of phase-3.

Figure 4b shows representative examples of type-2b debris. They are smaller in size, and appear to be segments of type-2c debris. Specifically, the structure of globules and columns is preserved but not the foam like appearance. In addition, globules interconnected with fibers indicate the separation from a more complex type-2c structure, arguably due to the higher pressure and lower viscosity at the time of their ejection. We thus assume that the ejection took place during mid-stage of phase-3 but the dynamic pressure (particle speed) was sufficiently low to maintain the globules and columns of the stretched-foam like structure of the superheated material during the separation of the particle.

The type-2a debris is formed early during phase-3 of the material ejection process when the temperature of the superheated material is higher (thus viscosity is lower) compared to the later stages of phase-3 when type-2b and type-2c particles are ejected. In addition, the speed of the particles is higher. The combination of lower viscosity and higher dynamic pressure can cause deformation of the particles during their flight in air. Typical examples of type-2a particles are shown in Figure 4a. They are observed to have a spherical outline with clearly visible globules but the foam like structure has been lost. Dangling and interconnecting fibers are also commonly observed that are often wrapped around the particle, a signature that the particle was rotating during its flight. We propose that the dynamic pressure has modified the shape of these particles causing the collapse of the foam like structure of the superheated material at the time of ejection. The size of the globules is also slightly smaller compared to the corresponding size of type-2b and type-2c particles, which is expected based on the lower viscosity of the superheated material. Indeed, as the periodicity of the structure of the superheated material during volume boiling (phase-3) may depend on the viscosity, the diameter of the globules (between 2 and 4 μm) and the interconnecting columns (between 0.5 and 2 μm) provides a signature.

Type-3 and type-4 debris arise from mechanical damage of the cold material surrounding the superheated region. The initial pressure inside the superheated material is on the order of 10 GPa which cause axial compressive stress of the surrounding cold material volume. A rarefaction wave is following the shockwave causing reduction of the medium's density which leads to circumferential (hoop) stress that support generation of radial cracks [18]. Release of the compressive stress eventually leads to axial tensile stress as the compressed material relaxes. This supports the generation of lateral cracks. This mechanism causes pulverizations of the surrounding material volume leading to generation of fragmentation particles. The particles are ejected in the presence of stored stress, which is released as the superheated material volume is relaxing. The difference between type-3 and type-4 debris is the location they originate. Type-3 debris originate at the boundary of the liquid material pool thus they contain molten material remnants. This aspect is illustrated in the representative images shown in Figure 5. Fibers having diameter between about 120 nm and 300 nm are commonly observed indicating that separation took place while the material was still in liquid phase.

Finally, type-4 debris originates from adjoining pulverized region. Typical examples are represented by the SEM images shown in Figure 6. Classic cleaved surfaces along with fragments that contained the polished surface of the substrate (example on right hand side in Figure 6) represent the typical morphology of type-4 debris.

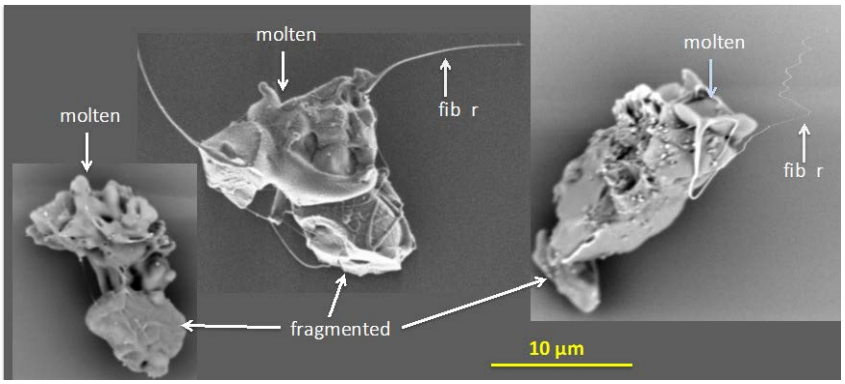

Figure 5. Representative SEM images of type-3 debris.

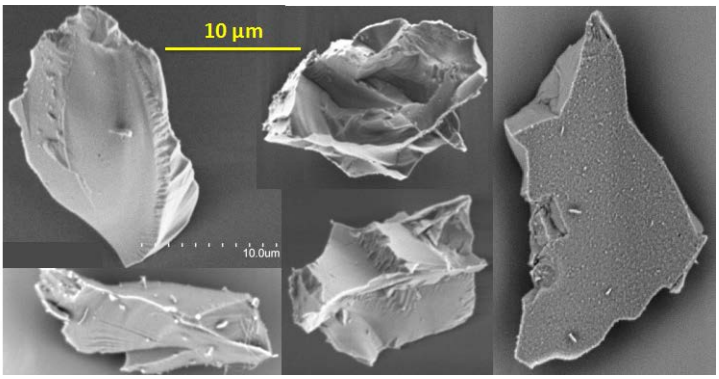

Figure 6. Representative SEM images of type-4 debris.

Although particles were typically observed to maintain their initial structure after impact on the collector substrate, areas on the collector sample surface that resembled a secondary debris zone around an impact location of a larger ejected particle were also infrequently observed. A typical example is shown in Figure 7. This secondary debris field (where fragments are at closed proximity with each other around the impact location) is comprised of fragments that do not resemble the appearance of any type of debris as discussed above. Instead, they encompass sharp edges and rough surfaces. We postulate that this type of fragments arises from the disintegration of larger type-2 particles having higher speed while their surface has nearly solidified upon impact. This causes the disintegration of the particle upon impact and the dispersion of fragments originating in the interior of the particle that rapidly solidify. Furthermore, upon closer observation of the impact area (see inset in Figure 7) it can be seen that the collector sample substrate has also incurred mechanical damage, with flakes protruding from the surface but pined down by the secondary debris.

4. DISCUSSION

This study provides direct information regarding the morphology of the generated debris. In turn, the morphologies of the produced debris provide a fingerprint of the state of the material during its relaxation. The shapes and sizes of the debris correlate to their location and time of ejection while the shape of the molten debris correlates with the transient viscosity and pressure of the superheated material. The "frozen" nodular and columnar features may be related to instabilities inside the superheated material during volume boiling. Such debris is expected to be generated during laser induced damage on silica optics used in ICF class laser systems. The experiments were designed to generate a larger volume of superheated material. This enabled the observation of larger ejected particles deemed as type-2c debris. Such debris may not be generated during laser induced damage initiation at ICF class laser operational conditions. However, it is well accepted that such laser systems operate with a number of "growing" damage sites during operation. These sites

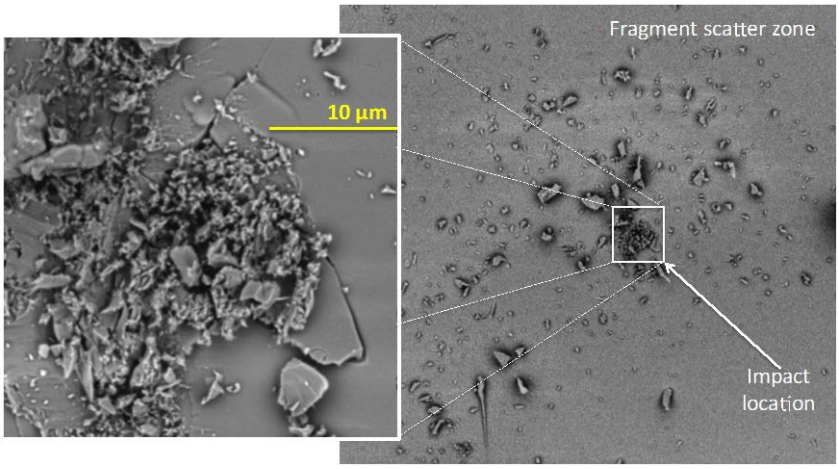

Figure 7. Images of impact location of type-2 debris providing evidence of mechanical damage on the surface of the collector sample

are absorbing sufficiently large amount of energy [17] to support formation of a larger pool of superheated material, thus generate type 2c debris.

The particles investigated in this work are ejected well after the termination of the laser pulse and they are associated with the intrinsic response of the material to its localized superheating. It is therefore expected that the generation of these particles is largely independent of the excitation conditions (laser energy, wavelength, pulse duration, excitation geometry). The dominant parameters are expected to be the spatial dimensions and the initial temperature and pressure of the superheated material volume which determines the relative contribution of each type of debris generated during the explosive relaxation of the material. In addition, the observed behaviors are not expected to be unique to fused silica. Instead, similar response is expected from other transparent solid state materials with adaptations related to the individual material thermo-physical and thermo-mechanical properties.

The results also suggest that the ejected particles having higher speeds can cause impact damage on adjacent optics. The presence of optical components at short separation distances is typical in ICF class laser systems. Furthermore, the section of the laser handling the higher laser harmonics (that are more susceptible to damage initiation and damage growth) is in a reduced pressure environment which would support the traversing of the particles from the one (damaging) optics to the neighboring optic with minimal kinetic energy loss. As a result, additional damage on the neighboring optic from impact in addition to contamination by the ejected particles is anticipated. The later can lead to new damage initiation and growth sites and be the origin of phase objects and light scattering centers [19].

ACKNOWLEDGEMENTS

This work was performed under the auspices of the U.S. Department of Energy by Lawrence Livermore National Laboratory under Contract DE-AC52-07NA27344. [LLNL-PROC-678399]

REFERENCES

[1] F. W. Dabby, U-C. Peak, IEEE J Quant. Electr. **8**, 106-111 (1972)
[2] Miotello, R. Kelly, Appl. Phys. A **69**, S67-S73 (1999)
[3] N.M. Bulgakova, A.V. Bulgakov**,** Appl. Phys. A **73**, 199–208 (2001)
[4] P. Lorazo, L. J. Lewis, Meunier, Lorazo, P. Lewis, M. Meunier, Phys. Rev. B **73**, 134108 (2006)
[5] E. Leveugle, A. Sellinger, J. M. Fitz-Gerald, L. V. Zhigilei, Phys. Rev. Lett. **98**, 216101 (2007)
[6] R. F. Wood, K. R. Chen, J. N. Leboeuf, A. A. Puretzky, and D. B. Geohegan, Phys. Rev. Lett. **79**, 1571-1574 (1999)
[7] S. S. Harilal, C. V. Bindhu, M. S. Tillack, F. Najmabadi, and A. C. Gaeris, J. Appl. Phys**. 93**, 2380 (2003)
[8] Z. Chen, A. Bogaerts, J. Appl. Phys. **97**, 063305 (2005)
[9] Q. Ma, V. Motto-Ros, Xueshi Bai, J. Yu, Appl. Phys. Lett. **103**, 204101 (2013)
[10] A. Salleo, S.T. Taylor, M.C. Martin, W.R. Panero, R. Jeanloz, T. Sands, and F.Y. Genin, Nat. Mater. **2**, 796 (2003).
[11] C. H. Li, X. Jua, J. Huang, X. D. Zhou, Z. Zheng, X. D. Jiang, W. D. Wu, and W. G. Zheng, Nucl. Instrum. Meth. B 269, 544 (2011).
[12] M. J. Matthews, C. W. Carr, H. A. Bechtel, and R. N. Raman, Appl. Phys. Lett. **99**, 151109 (2011).
[13] S. G. Demos, R. A. Negres, R. N. Raman, M. D. Feit, K. R. Manes, A. M. Rubenchik, Optica 2, 765-772 (2015)
[14] R.N. Raman, S. Elhadj, R. A. Negres, M. J. Matthews, M. D. Feit, and S. G. Demos, Opt. Express **20**, 27720 (2012).
[15] R. H. Doremus, J. Appl. Phys. 92, 7619–7629 (2002)
[16] R. N. Raman, R. A. Negres, and S. G. Demos, . Appl. Phys. Lett. **98**, 051901 (2011)
[17] S. G. Demos, R. N. Raman R. A. Negres , Optics Express **21**, 4875 (2013)
[18] S. G. Demos, R. A. Negres, R. N. Raman, A. M. Rubenchik, M. D. Feit, Laser Photon. Rev **7**, 444-452 (2013)
[19] M. J. Matthews, N. Shen, J. Honig, J. D. Bude, and A. M. Rubenchik, J. Opt. Soc. Am. B **30**, 3233-3242 (2013).